

# Calcium Ions Are Involved in the Unusual Red-Shift of the Light-Harvesting 1 $Q_y$ Transition of the Core Complex in Thermophilic Purple Sulfur Bacterium *Thermochromatium tepidum*\*

Yukihiro Kimura<sup>1,§</sup>, Yu Hirano<sup>1</sup>, Long-Jiang Yu<sup>1</sup>, Hiroaki Suzuki<sup>1</sup>, Masayuki Kobayashi<sup>2</sup>, and Zheng-Yu Wang<sup>1,†</sup>

<sup>1</sup>Faculty of Science, Ibaraki University, Mito 310-8512, Japan and <sup>2</sup>Ariake National College of Technology, Omuta, Fukuoka 836-8585, Japan.

Running Title:  $Ca^{2+}$ -binding to the LH1 complex of *Tch. tepidum*

<sup>†</sup>Correspondence should be addressed: Tel/Fax +81-29-228-8352; e-mail: wang@mx.ibaraki.ac.jp

Thermophilic purple sulfur bacterium, *Thermochromatium tepidum*, can grow at temperatures up to 58 °C and exhibits an unusual  $Q_y$  absorption at 915 nm for the core light-harvesting complex (LH1), about 35 nm red-shift from those of its mesophilic counterparts. We demonstrate in this study, using a highly purified LH1-reaction center complex, that the LH1  $Q_y$  transition is strongly dependent on metal cations and  $Ca^{2+}$  is involved in the unusual red-shift. Removal of the  $Ca^{2+}$  resulted in formation of a species with the LH1  $Q_y$  absorption at 880 nm, and addition of the  $Ca^{2+}$  to the 880-nm species recovered the native 915-nm form. Interchange between the two forms is fully reversible. Based on spectroscopic and isothermal titration calorimetry analyses, the  $Ca^{2+}$ -binding to the LH1 complex was estimated to occur in a stoichiometric ratio of  $Ca^{2+}/\alpha\beta$ -subunit = 1:1 and the binding constant was in  $10^5 M^{-1}$  order of magnitude, which is comparable with those for EF-hand  $Ca^{2+}$ -binding proteins. Despite the high affinity, conformational changes in the LH1 complex upon  $Ca^{2+}$ -binding were small and occurred slowly with a typical time constant of about 6 minutes. Replacement of the  $Ca^{2+}$  with other metal cations caused blue-shifts of the  $Q_y$  bands depending on the property of the cations, indicating that the binding site is highly selective. Based on the amino acid sequences of the LH1 complex, possible  $Ca^{2+}$ -binding sites are proposed, which consists of several acidic amino acid residues near the membrane interfaces of the C-terminal region of the  $\alpha$ -polypeptide and the N-terminal region of the  $\beta$ -polypeptide.

*Thermochromatium (Tch.) tepidum* is a thermophilic purple sulfur photosynthetic bacterium, which can grow at temperatures up to 58 °C, the highest known for purple bacteria (1, 2). The crystal structure of the reaction center (RC)<sup>1</sup> for this bacterium has been determined (3), revealing structural features similar to those of the RCs from other purple bacteria (4, 5). The antenna system in *Tch. tepidum* contains two types of light-harvesting complex, LH1 and LH2. The LH1 complex has been shown to be tightly associated with RC to form the core complex (6, 7), LH1-RC, and the LH2 complex is supposed to be located in the periphery of the core complex (8, 9). Although a number of high-resolution structures are available for the LH2 and LH3 (a spectroscopic variant of LH2) complexes (10-12), information on the molecular structure of the LH1 complex has been lacking. This information is essential for studying its biological functions in terms of excitation energy transfer and reduced ubiquinone transport. The interaction mode between LH1 and RC complexes is also of particular interest because the RC has a structure of 2-fold symmetry (3, 4, 13), whereas low resolution structures of LH1 show a pseudo 14 or 16-fold symmetry depending on the species (14-20). The symmetry issue needs to be taken into account when addressing the possible contacting sites between the LH1 and RC, and the factors determining the specific orientation of RC inside the LH1 ring. The crystallographic structure of the LH1-RC complex from *Rhodospseudomonas (Rps.) palustris* at 4.8 Å resolution shows a slightly elliptical LH1 ring composed of 15 pairs of the  $\alpha\beta$ -polypeptides with a gap that is associated with an unknown protein W and is

proposed to be adjacent to the ubiquinone binding site in RC (17). However, to gain insight into a more detailed picture of the configuration of LH1-RC, structural information at higher resolutions is required. Recently, the LH1-RC complex from *Tch. tepidum* has been crystallized (21).

We have shown that the purified LH1-RC complex of *Tch. tepidum* is extremely stable (21, 22). Beside the thermal stability, another striking feature is the unusual red-shift of the  $Q_y$  transition of the LH1 complex. Although the core complex contains only *a*-type bacteriochlorophyll (BChl), the same as those found in most other purple bacteria, spectroscopically the LH1 complex of *Tch. tepidum* exhibits a  $Q_y$  absorption at 915 nm, about 35 nm red-shifted from those of its mesophilic counterparts. The reason for this red-shift has been unclear (2). Two other LH1 complexes from purple bacteria strain 970 and *Roseospirillum parvum* 930I were reported to exhibit  $Q_y$  absorptions at 963 nm (23) and 909 nm (24, 25), respectively. The large red-shifts were explained in terms of enhanced exciton interaction among the BChl *a* molecules and specific interactions between BChl *a* and LH1 polypeptides. Recent studies on the LH complexes show that small differences in the primary structure of the apoproteins can alter the spectroscopic properties (12, 26-29). The hydrogen bonding pattern and local environment were shown to have an effect on the conformation of the coupled BChl *a* molecules, and small changes in the conformation could result in a significant shift of the  $Q_y$  transition.

In a preliminary study, we found that the LH1  $Q_y$  absorption of *Tch. tepidum* core complex appeared to be affected by various cations used in the experiment (6). However, the LH1-RC samples used in the previous work were partially damaged, and the LH2 along with other two unknown proteins were not completely removed. We demonstrate in the present work using highly purified samples that the calcium ions are strongly involved in the unusual red-shift of the LH1  $Q_y$  transition. A species with absorption maximum at 880 nm can be obtained from the LH1 915-nm complex by removing the  $Ca^{2+}$ , and the native LH1 915-nm form (B915) can be recovered from the 880-nm species (B880) by addition of  $Ca^{2+}$ . Interchange between the two forms is reversible. Effects of the  $Ca^{2+}$  on the properties of the LH1-

RC complex from *Tch. tepidum* are analyzed by absorption, circular dichroism (CD) spectroscopies, isothermal titration calorimetry (ITC), and sucrose density gradient ultracentrifugation analyses. The  $Ca^{2+}$ -binding constants are estimated both spectroscopically and thermodynamically. The rates of conformational changes upon the  $Ca^{2+}$ -binding are calculated from a pseudo first-order kinetics analysis. By comparison of the amino acid sequences of LH1 complexes, possible  $Ca^{2+}$ -binding sites are proposed. The  $Ca^{2+}$ -dependent spectral behavior of the LH1 complex has not been reported for other purple photosynthetic bacteria, and is of great interest and significance in understanding the structural and functional roles of  $Ca^{2+}$  in this thermophilic organism.

## MATERIALS AND METHODS

### *Sample Preparation.*

Cells from *Tch. tepidum* were cultured anaerobically at 48 °C for 7 days as described previously (7). Isolation and purification followed the same procedure described before (21) except that *n*-octyl- $\beta$ -D-glucopyranoside (OG) was used as detergent in solubilization and chromatography. The harvested cells were disrupted by sonication in 20 mM Tris-HCl buffer at pH 8.5. Chromatophores were first treated with 0.35% (w/v) lauryldimethylamine *N*-oxide at 25 °C for 60 min followed by centrifugation at 150,000  $\times g$  for 90 min. The pellet was further treated with 1.0% (w/v) OG and centrifuged at 150,000  $\times g$  for 90 min to extract the LH1-RC components. The supernatant was loaded onto a DEAE anion-exchange column (Toyopearl 650S, TOSOH) equilibrated at 4 °C with 20 mM Tris-HCl buffer (pH 7.5) containing 0.8% (w/v) OG. The LH1-RC fraction was eluted by a linear gradient of NaCl from 50 mM to 125 mM, and peak fractions with a ratio of  $A_{915}/A_{280}$  over 2.10 were collected.

The native LH1-RC complex was passed through a size exclusion column (Sephadex G25M PD10, GE Healthcare) to remove excess salts, followed by incubation at 0 °C for 3 hrs in darkness in the presence of 1.25 mM ethylenediamine tetraacetic acid (EDTA,

trisodium, salt). The sample solution was extensively washed with a buffer containing 20 mM Tris-HCl (pH 7.5) and 0.8% OG to remove excess of EDTA. The final concentration of EDTA in the solution was estimated to be lower than 1 nM. The resulting core complex showed a LH1  $Q_y$  absorption maximum around 880 nm. To examine the effects of metal cations, the B880 sample was incubated at 0 °C overnight after adding various metal cations.

Sucrose density gradient centrifugation analysis was conducted by the ultracentrifugation at  $150,000 \times g$  and 4 °C for 12 hrs under a 10 – 40 % (w/v) continuous gradient of sucrose concentration in a buffer containing 20 mM Tris-HCl (pH 7.5) and 0.7% (w/v) OG in the presence or absence of 1 mM EDTA.

#### *Spectroscopic Measurements*

Absorption spectra were recorded on a Beckman DU-640 spectrophotometer at room temperature. Kinetic analysis for the recovering process from B880 to B915 upon the addition of  $Ca^{2+}$  was performed by monitoring the increase of the absorbance at 937 nm. Circular dichroism (CD) spectra were recorded on a Jasco J-720w spectropolarimeter in the ranges of 200 – 300 nm and 400 – 1000 nm. The measurements were conducted under the conditions of 20 nm/min of scan speed, 1.0 nm of bandwidth, and 2 sec of response time. For the CD measurement between 200 – 300 nm, data were averaged over 10 scans in order to improve the signal-to-noise ratio, while for the measurements between 400 – 1000 nm the spectra were obtained from one scan. The molar extinction coefficient of BChl *a* dimer in a native  $\alpha\beta$ -subunit was estimated to be  $270 \text{ mM}^{-1} \text{ cm}^{-1}$  by extracting BChl *a* molecules from purified LH1-RC complexes with acetone/methanol (7/2, v/v) and using  $\epsilon_{770} = 76 \text{ mM}^{-1} \text{ cm}^{-1}$  for the monomeric BChl *a* (30).

#### *Isothermal Titration Calorimetry (ITC)*

ITC measurements were carried out on a MicroCal VP-ITC microcalorimeter (MicroCal Inc.) at 25 °C. The LH1-RC samples were dissolved in 20 mM Tris-HCl (pH 7.5) and 0.7% OG at 250  $\mu\text{M}$ . Following thermal equilibration at 25 °C, a total of 14 injections of 50 mM  $CaCl_2$

dissolved in the same buffer were made in 1  $\mu\text{l}$  aliquots into the cell from the syringe using a 300 r. p. m. stirring speed. An injection delay of 10 minutes was utilized to allow for the baseline to return after each injection. The titration data were deconvoluted based on a binding model containing either one or two sets of noninteracting binding sites by a nonlinear least squares minimization method (31) performed using the MicroCal Origin ITC software.

## RESULTS

First we confirmed the effect of various metal cations on the absorption spectrum using highly purified LH1-RC complex from the *Tch. tepidum* (Fig. S1 in Supplemental Data). The native core complex (B915) exhibited LH1  $Q_y$  absorption at 914 nm as reported previously (21). The  $Q_y$  band was retained at the original position only in the presence of  $Ca^{2+}$ , and blue-shifted by the addition of other cations. The results indicate that the native LH1 form of the *Tch. tepidum* is sensitive to the coexisting metal cations.

To investigate whether the B915 species is bound to metal ions, metal chelators were employed. Figure 1 shows an absorption spectrum obtained with the addition of EDTA to the B915 species. The LH1  $Q_y$  band was largely blue-shifted to 876 nm with a spectral shape similar to those observed for the LH1 complexes from other purple bacteria. This clearly indicates that metal ions are involved in the formation of the B915, and removal of the cation by EDTA results in a conformational change of the BChl *a* molecules in the LH1 complex, leading to a large blue-shift of the LH1  $Q_y$  band. Similar results were observed using different metal chelators, nitrilotriacetic acid and ethylene glycol-bis( $\beta$ -aminoethyl ether)-*N, N, N', N'*-tetraacetic acid (tetrasodium salt), suggesting that the blue-shift was not caused by the specific interaction between EDTA and the core complex. We further investigated the effects of various cations on the EDTA-treated LH1-RC complex (B880). Typical results on the divalent cations are shown in Fig. 1, and the results for monovalent cations are provided in Supplemental Data (Fig. S2). Red-shifts with respect to the LH1  $Q_y$  band (876 nm) of the B880 species were observed with additions of all cations. Among the divalent cations tested, only  $Ca^{2+}$  gave an absorption

spectrum closely resembling that of native B915 species with the LH1  $Q_y$  absorption maximum at 913.5 nm. Addition of other cations resulted in small red-shifts of the LH1  $Q_y$  band to 885 nm – 889 nm for the divalent cations and 879 nm – 884 nm for the monovalent cations, respectively. The results strongly suggest that the B915 species is induced from the B880 species by the binding of  $\text{Ca}^{2+}$  to the LH1 complex.

The binding property of  $\text{Ca}^{2+}$  was examined over a wide range of  $\text{Ca}^{2+}$  concentration. Figure 2 shows the absorption spectra of the EDTA-treated core complex in the presence of  $\text{Ca}^{2+}$  at various concentrations. With increasing the  $\text{Ca}^{2+}$  concentration, the B915 species was formed accompanying by a decrease of the B880 species. There was an isosbestic point at 895 nm, indicating that the B915 was recovered from the B880 upon the addition of  $\text{Ca}^{2+}$ . The  $\text{Ca}^{2+}$ -dependent LH1  $Q_y$  shifts were plotted in the inset as a function of the  $\text{Ca}^{2+}$  concentration, revealing a sigmoid curve that saturated around 50  $\mu\text{M}$  of  $\text{Ca}^{2+}$ . Kinetics of the  $\text{Ca}^{2+}$ -binding process at room temperature (25 °C) was analyzed using the pseudo first-order model. Formation of the B915 species was monitored at 937 nm where we can observe the maximum change in the intensity. Figure 3 shows the time profile of the absorption change ( $\Delta A$ ) after addition of 5 mM  $\text{Ca}^{2+}$  to the B880 species of 7  $\mu\text{M}$  LH1 subunit. The absorbance at 937 nm increased with time and reached maximum in about 30 min. Since the concentration of  $\text{Ca}^{2+}$  was much higher than that of the B880 species, the binding process can be represented by a pseudo first-order kinetics model. The time-dependent absorption change  $\Delta A(t)$  can be expressed by the first-order rate equation as shown in Eq. 1,

$$\Delta A(t) = \Delta A \times [1 - \exp(-k \times t)] \quad (\text{Eq. 1})$$

where  $\Delta A$  is the final change of absorbance at 937 nm,  $k$  is the rate constant for the conformational change of the LH1 complex upon the  $\text{Ca}^{2+}$ -binding, and  $t$  is the time in minutes after the addition of  $\text{Ca}^{2+}$ . By a least-square fitting of the data using Eq. 1, the rise rate constant  $k$  of B915 was determined to be 0.20  $\text{min}^{-1}$ . This value did not change very much over a range of 2.5 mM to 100 mM of the  $\text{Ca}^{2+}$  concentration (Fig. 3, inset),

suggesting that the pseudo first-order kinetic analysis is valid and the conformational changes from B880 to B915 upon the  $\text{Ca}^{2+}$ -binding occur slowly under the experimental conditions.

The binding affinity of  $\text{Ca}^{2+}$  to B880 was evaluated by a nonlinear least-square fitting of the spectroscopic data. Figure 4 shows the plots of  $\Delta A$  at several wavelengths between 930 nm – 960 nm as a function of the  $\text{Ca}^{2+}$  concentration. These wavelengths were selected so as to minimize contribution from the RC that has absorption over 750 nm – 950 nm. Assuming that one LH1 subunit of the B880 species binds to one  $\text{Ca}^{2+}$  to form one subunit of the B915 species, the absorption changes  $\Delta A$  observed can be expressed by the following equation (see Supplemental Data for details),

$$\Delta A = l \times (\varepsilon_{915} - \varepsilon_{880}) \times [(1 + C_0K + Kx) - \{(1 + C_0K + Kx)^2 - 4C_0K^2x\}^{0.5}]/2K \quad (\text{Eq. 2})$$

where  $l$  is the light-path length,  $\varepsilon_{915}$  and  $\varepsilon_{880}$  are molar extinction coefficients of the LH1 subunit in the B915 and B880 forms, respectively,  $C_0$  is the initial concentration of subunit of the B880 species,  $K$  is the  $\text{Ca}^{2+}$ -binding constant, and  $x$  is the concentration of  $\text{Ca}^{2+}$ . By using the nonlinear least-square fitting of  $\Delta A$ , the  $\text{Ca}^{2+}$ -binding constant  $K$  was estimated to be  $6.5 (\pm 0.3) \times 10^5 \text{ M}^{-1}$ . Figure 4 shows a good agreement between the calculated result and the spectroscopic data. The value of the binding constant is comparable to those reported for typical EF-hand  $\text{Ca}^{2+}$ -binding proteins (32).

The binding properties of  $\text{Ca}^{2+}$  to the LH1 complex were further examined by a thermodynamic analysis. Figure 5A shows the ITC profile obtained with titration of  $\text{Ca}^{2+}$  to the B880 species. Large exothermic change was observed for each injection, providing an independent evidence for the strong  $\text{Ca}^{2+}$ -binding. A remarkable feature in the thermogram is that each exothermic signal clearly revealed a two-phase change: a rapid return immediately after the injection and a slow recovery followed, as shown typically in the inset of Fig. 5A. The two exothermic components can be interpreted in terms of a fast  $\text{Ca}^{2+}$ -binding to the B880 and a slow process of conformational rearrangement within the core complex, respectively. Based on

a two-component analysis, the time constants were determined to be 20 sec and 369 sec for the fast and slow processes, respectively. The latter is quite consistent with the rate constant observed from spectroscopic measurement (Fig. 3). Figure 5B shows a plot of the integrated heat per mol of injectant ( $\text{Ca}^{2+}$ ) as a function of the molar ratio of  $\text{Ca}^{2+}/(\text{B880 subunit})$ . The plot exhibited a sigmoid-like curve with a stoichiometrically equivalent point around 1.0, suggesting that the  $\text{Ca}^{2+}$ -binding phenomenon can be described by a simple one-site model. From the model analysis, several thermodynamic parameters were obtained: the number of binding site per subunit  $N = 0.97$ , the binding constant  $K = 9.6 \times 10^4 \text{ M}^{-1}$ , and enthalpy change  $\Delta H = -4.0 \text{ kcal mol}^{-1}$ . Using these values, the changes of Gibbs free energy  $\Delta G$  and entropy  $\Delta S$  were evaluated to be  $-6.8 \text{ kcal mol}^{-1}$  and  $9.36 \text{ cal mol}^{-1} \text{ K}^{-1}$ , respectively, from the following equation,

$$\Delta G = \Delta H - T\Delta S = -nRT \ln K \quad (\text{Eq. 3})$$

where  $T$  is the absolute temperature,  $n$  is the mole number, and  $R$  is the gas constant,  $8.315 \text{ J mol}^{-1} \text{ K}^{-1}$ . These thermodynamic parameters indicate that the  $\text{Ca}^{2+}$ -binding site has a high affinity with a 1:1 stoichiometric ratio and the  $\text{Ca}^{2+}$ -binding is driven both enthalpically and entropically.

Structural differences in conformation and assembly of the core complexes between the B915 and B880 species were investigated by CD spectroscopy and sucrose density gradient centrifugation. Figure 6 shows the CD spectra. As reported previously, the CD spectrum of B915 was characterized by small and nonconservative signals in the  $Q_y$  region (21), a typical feature for the core complexes from purple bacteria (33, 34). Upon removal of  $\text{Ca}^{2+}$ , the CD signals for the  $Q_y$  and  $Q_x$  bands were blue-shifted in accordance with the changes of absorption spectra, whereas other signals from the RC and carotenoids remained unchanged. These results support that  $\text{Ca}^{2+}$ -dependent spectral changes originate from the change in configuration of the BChl  $a$  molecules in the LH1 complex. We also examined the effect of  $\text{Ca}^{2+}$  on the secondary structure of the apoproteins of the LH1-RC complex by measuring the CD spectra in far UV region (Fig. 6 inset). Both spectra for the B915 and B880 revealed almost the same shape and can be characterized by

highly  $\alpha$ -helical structures. This suggests that there was no change in the secondary structures of the polypeptides. Sucrose density gradient ultracentrifugation exhibited a single band for both B915 and B880 at identical position (Fig. S3 in Supplemental Data), indicating that the B880 is not a decomposed form of B915 and the whole assembly of the core complex remains unchanged.

All results described above were obtained using the purified LH1-RC complex. In Fig. 7, we show that similar phenomena can be observed for *Tch. tepidum* chromatophores. The chromatophore membrane contains a large amount of LH2 complex, as revealed by the intensive absorption maxima at 800 and 850 nm, and a small amount of LH1 complex with the  $Q_y$  transition at 915 nm. In the presence of  $\text{CaCl}_2$ , there was no change in the absorption spectrum of the chromatophore. However, upon the addition of EDTA or  $\text{MgCl}_2$ , the LH1 915-nm band was shifted toward 880 nm and merged with the LH2 absorptions. The result implied that the  $\text{Ca}^{2+}$ -binding site of the LH1 complex exists in a hydrophilic part or at the membrane interface where metal cations and EDTA are readily accessible.

## DISCUSSION

The present study demonstrated that the LH1  $Q_y$  transition at 915 nm of the core complex from *Tch. tepidum* is induced by the binding of  $\text{Ca}^{2+}$  to the LH1 complex. Removal of the  $\text{Ca}^{2+}$  resulted in a blue-shift of the LH1  $Q_y$  transition to 876 nm, the wavelength similar to those of other mesophilic purple bacteria. The B915 native form can be recovered from the B880 by the addition of  $\text{Ca}^{2+}$ . The result indicates that  $\text{Ca}^{2+}$  is an indispensable cofactor for retaining the native structure of the *Tch. tepidum* LH1 complex. The  $\text{Ca}^{2+}$ -binding property of the *Tch. tepidum* LH1 complex is considered to be closely related to the living environment of this organism. Mammoth Hot Springs in Yellowstone National Park, from where the bacterium was collected (1), is known to contain rich mineral calcium carbonate deposited over millions of years to form thick layers of sedimentary limestone (see <http://www.nps.gov/archive/yell/features/mammothour/>). This bacterium can not grow in a  $\text{Ca}^{2+}$ -depleted culture (data not shown).

Through the spectroscopic and ITC analyses, binding of the  $\text{Ca}^{2+}$  to the LH1  $\alpha\beta$ -subunit was found to occur in a one-to-one ratio with a binding constant of approximately  $10^5$  order of magnitude. The high binding affinity is comparable with that for the well-known EF-hand  $\text{Ca}^{2+}$ -binding proteins (32, 35). Generally,  $\text{Ca}^{2+}$  is classified as a hard acid and prefers to interact with a hard base. In the proteins with an EF-hand  $\text{Ca}^{2+}$ -binding site, the ligands are mainly composed of oxygen atoms from acidic amino acid residues (Asp and Glu) as well as those from main chain carbonyl groups and water molecules (35). Inspection of the primary sequences of the *Tch. tepidum* LH1 polypeptides revealed that three Asp in the  $\alpha$ -polypeptide are located in the C-terminal region and are close to the BChl *a*-coordinating His residue (Fig. 8) (6, 7). Three similar residues (two Glu and one Asp) are also found in the C-terminus of the LH1  $\alpha$ -polypeptide from the mesophilic purple bacterium *Allochrochromatium (Ach.) vinosum*. However, a deletion exists in this region of the *Tch. tepidum* LH1  $\alpha$ -polypeptide, which is thought to be essential for the formation of a  $\text{Ca}^{2+}$ -binding site and the specific interaction between the polypeptide and pigment molecule. Positions of the deletion and the three Asp residues are estimated to be on the membrane interface or in the hydrophilic part of the  $\alpha$ -polypeptide. Similarly, several neighboring acidic residues are found in the N-terminal domain of the  $\beta$ -polypeptide, which might also serve as a potential binding site. Possibilities for other residues around the BChl *a*, which are capable of hydrogen-bonding (27, 29) and/or  $\text{Ca}^{2+}$ -binding, need to be further investigated.

Despite the high affinity between the *Tch. tepidum* LH1 complex and  $\text{Ca}^{2+}$ , the structural changes induced by the  $\text{Ca}^{2+}$ -binding occurred slowly as revealed from the spectroscopic and the ITC measurements. Therefore, the conformational change from B880 to B915 is the rate limiting step under the experimental conditions. Previous study showed that the *Tch. tepidum* LH1-RC complex was purified in a monomeric form with the LH1 ring composed of 16  $\alpha\beta$ -subunits (21). In the present work, the  $\text{Ca}^{2+}$ -binding to the LH1 complex was estimated to occur in a stoichiometric ratio of  $\text{Ca}^{2+}/\alpha\beta$ -subunit=1:1. This means that the B915 form

may not be completed from the B880 form until all the 16 binding sites are occupied by the  $\text{Ca}^{2+}$  ions, because the  $Q_y$  transition is a consequence of cooperative interaction between the exciton states formed by the 32 BChl *a* molecules. In the case where there are less  $\text{Ca}^{2+}$  ions than LH1- $\alpha\beta$  pairs, original state of the exciton interaction in the LH1 ring will be altered and become heterogeneous. As a result, a broadening in the  $Q_y$  transition could be expected. Such broadening was actually observed at low  $\text{Ca}^{2+}$  concentrations up to 3.2  $\mu\text{M}$  (Fig. 2 and Fig. S4 in Supplemental Data). At higher  $\text{Ca}^{2+}$  concentrations than 3.2  $\mu\text{M}$ , the full width at half maximum (FWHM) decreased rapidly with increasing the  $\text{Ca}^{2+}$  concentration. Taking into account the total molecular weight of about 330,000 for the core complex, the slow structural change may be interpreted in terms of the large size of the membrane proteins associated with a considerable amount of the surrounded detergent molecules. Other factors include that a relatively long time is required for the fine tuning of the 16  $\text{Ca}^{2+}$ -bound  $\alpha\beta$ -subunits within the LH1 complex to form a stabilized conformation which can also contribute to the thermal stability of the *Tch. tepidum*.

Generally, metal binding to proteins is known to be driven entropically because the dehydration enthalpy of divalent cations is highly endothermic. However, overall enthalpy could become exothermic if the metal binding is thermodynamically coupled to the conformational change which eventually could result in a thermal stabilization of the protein (36). In calmodulins from bovine brain (37-39) and wheat germ (40), the  $\text{Ca}^{2+}$ -binding reactions were reported to be driven solely by a large favorable entropy change despite unfavorable enthalpy change. In contrast, for the troponin C (41-43) and parvalbumins (32, 44, 45) the  $\text{Ca}^{2+}$ -binding reactions were mostly favorable in both entropy and enthalpy except for several specific sites where endothermic and entropy-driven reactions occur in a similar way to the calmodulins (42-44). For the *Tch. tepidum* LH1-RC complex, the  $\text{Ca}^{2+}$ -binding is driven both entropically and enthalpically, similar to the cases of troponin C and parvalbumins. Therefore, the large exothermic changes of the *Tch. tepidum* core complex strongly support that the  $\text{Ca}^{2+}$ -binding to LH1 complex caused a conformational change that

largely stabilized the structure of the LH1-RC complex.

The  $\text{Ca}^{2+}$ -binding in calmodulins was reported to induce a conformational transition of random coils to  $\alpha$ -helical structures based on the results of CD measurement (46-48). For the *Tch. tepidum* core complex, the far UV-CD spectra did not show any change in the  $\text{Ca}^{2+}$ -depletion. This means that conformational change of LH1 complex may occur mainly in the tertiary structure, or the change in the secondary structure, if there is, may be too small to be detected. Similar results were reported for troponin C from rabbit skeletal muscle (41). In EF-hand proteins (35), the  $\text{Ca}^{2+}$ -binding sites are located in the loop of a helix-loop-helix motif and large conformational changes are accompanied with the binding of  $\text{Ca}^{2+}$ . In contrast, the putative  $\text{Ca}^{2+}$ -binding sites in the LH1 complex are located at the terminal regions of the polypeptides. Furthermore, the number of acidic residues involved in the binding site and their arrangement seem to be different from those of EF-hand  $\text{Ca}^{2+}$ -binding proteins (32). As a result, the slight structural change in LH1 can only be detected by its  $Q_y$  transition that is extremely sensitive to the conformational change of the BChl

*a* molecules. The changes in LH1  $Q_y$  transition for different alkaline earth cations appeared to be partly related to the ionic radius, as the cations with larger ( $\text{Sr}^{2+}$ ,  $\text{Ba}^{2+}$ ) and smaller ( $\text{Mg}^{2+}$ ) ionic radii than that of  $\text{Ca}^{2+}$  showed the cation dependent  $Q_y$  bands between 885 nm and 889 nm. However, substitution of  $\text{Cd}^{2+}$  that has an ionic radius almost the same as that of  $\text{Ca}^{2+}$  also induced a red-shift to 887 nm. The results indicate that the  $\text{Ca}^{2+}$ -binding site in the LH1 complex is highly selective and can distinguish the cations not only by the ionic radius but also by other properties such as binding mode and coordination number (49) as well as the hard-soft nature. In this regard, the complex mechanism of molecular recognition of the *Tch. tepidum* LH1 is expected to be explored by detailed structural information, and the effort toward determining a high-resolution structure of the core complex is in progress (21).

#### ACKNOWLEDGMENT

We thank Dr. J. Nakamura and Dr. Y. Sakaguchi of Nihon SiberHegner K.K. for the ITC measurements, and Mr. M. Nakamura, and Mr. K. Horiguchi for their technical assistance.

#### REFERENCES

1. Madigan, M. T. (1984) *Science* **225**, 313-315
2. Madigan, M. T. (2003) *Photosynth. Res.* **76**, 157-171
3. Nogi, T., Fathir, I., Kobayashi, M., Nozawa, T., and Miki, K. (2000) *Proc. Natl. Acad. Sci. USA* **97**, 13561-13566
4. Deisenhofer, J., Epp, O., Miki, K., Huber, R., and Michel, H. (1984) *J. Mol. Biol.* **180**, 385-398
5. Allen, J. P., Feher, G., Yeates, T. O., Komiya, H., and Rees, D. C. (1987) *Proc. Natl. Acad. Sci. USA* **84**, 5730-5734
6. Fathir, I., Ashikaga, M., Tanaka, K., Katano, T., Nirasawa, T., Kobayashi, M., Wang, Z.-Y., and Nozawa, T. (1998) *Photosynth. Res.* **58**, 193-202
7. Wang, Z.-Y., Shimonaga, M., Suzuki, H., Kobayashi, M., and Nozawa, T. (2003) *Photosynth. Res.* **78**, 133-141
8. Nozawa, T., Fukuda, T., Hatano, M., and Madigan, M. T. (1986) *Biochim. Biophys. Acta* **852**, 191-197
9. Kramer, H., and Ames, J. (1996) *Photosynth. Res.* **49**, 237-244
10. McDermott, G., Prince, D. M., Freer, A. A., Hawthornthwaite-Lawless, A. M., Papiz, M. Z., Cogdell, R. J., and Isaac, N. W. (1995) *Nature* **374**, 517-521
11. Koepke, J., Hu, X., Muenke, C., Schulten, K., and Michel, H. (1996) *Structure* **4**, 581-597

12. McLuskey, K., Prince, S. M., Cogdell, R. J., and Isaac, N. W. (2001) *Biochemistry* **40**, 8783-8789
13. Allen, J. P., Feher, G., Yeates, T. O., Rees, D. C., Deisenhofer, J., Michel, H., and Huber, R. (1986) *Proc. Natl. Acad. Sci. USA* **83**, 8589-8593
14. Karrasch, S., Bullough, P. A., and Ghosh, R. (1995) *EMBO J.* **14**, 631-638
15. Jungas, C., Ranck, J.-L., Rigaud, J.-L., Joliot, P., and Vermeglio, A. (1999) *EMBO J.* **18**, 534-542
16. Jamieson, S. J., Wang, P., Qian, P., Kirkland, J. Y., Conroy, M. J., Hunter, C. N., and Bullough, P. A. (2002) *EMBO J.* **21**, 3927-3935
17. Roszak, A. W., Howard, T. D., Southall, J., Gardiner, A. T., Law, C. J., Isaac, N. W., and Cogdell, R. J. (2003) *Science* **302**, 1969-1972
18. Scheuring, S., Seguin, J., Marco, S., Levy, D., Robert, B., and Rigaud, J.-L. (2003) *Proc. Natl. Acad. Sci. USA* **100**, 1690-1693
19. Scheuring, S., Francia, F., Busselez, J., Melandris, B. A., Rigaud, J.-L., and Levy, D. (2004) *J. Biol. Chem.* **279**, 3620-3626
20. Qian, P., Hunter, C. N., and Bullough, P. A. (2005) *J. Mol. Biol.* **349**, 948-960
21. Suzuki, H., Hirano, Y., Kimura, Y., Takaichi, S., Kobayashi, M., Miki, K., and Wang, Z.-Y. (2007) *Biochim. Biophys. Acta* **1767**, 1057-1063
22. Kobayashi, M., Fujioka, Y., Mori, T., Terashima, M., Suzuki, H., Shimada, Y., Saito, T., Wang, Z.-Y., and Nozawa, T. (2005) *Biosci. Biotechnol. Biochem.* **69**, 1130-1136
23. Permentier, H. P., Neerken, S., Overmann, J., and Ames, J. (2001) *Biochemistry* **40**, 5573-5578
24. Glaeser, J., and Overmann, J. (1999) *Arch. Microbiol.* **171**, 405-416
25. Tuschat, C., Beatty, J. T., and Overmann, J. (2004) *Photosynth. Res.* **81**, 181-199
26. Fowler, G. J. S., Visschers, R. W., Grief, G. G., van Grondelle, R., and Hunter, C. N. (1992) *Nature* **355**, 848-850
27. Olsen, J. D., Sockalingum, G. D., Robert, B., and Hunter, C. N. (1994) *Proc. Natl. Acad. Sci. USA* **91**, 7124-7128
28. Sturgis, J. N., Jirsakova, V., Reiss-Husson, F., Cogdell, R. J., and Robert, B. (1995) *Biochemistry* **34**, 517-523
29. Cogdell, R. J., Howard, T. D., Isaac, N. W., McLuskey, K., and Gardiner, A. T. (2002) *Photosynth. Res.* **74**, 135-141
30. Clayton, R. K., and Clayton, B. J. (1981) *Proc. Natl. Acad. Sci. USA* **78**, 5583-5587
31. Schwarz, F. P., Puri, K. D., Bhat, R. G., and Suroolia, A. (1993) *J. Biol. Chem.* **268**, 7668-7677
32. Ogawa, Y., and Tanokura, M. (1986) *J. Biochem.* **99**, 81-89
33. Georgakopoulou, S., van Grondelle, R., and van der Zwan, G. (2006) *J. Phys. Chem. B* **110**, 3344-3353
34. Georgakopoulou, S., van Grondelle, R., and van der Zwan, G. (2006) *J. Phys. Chem. B* **110**, 3354-3361
35. Grabarek, Z. (2006) *J. Mol. Biol.* **359**, 509-525
36. Yamniuk, A. P., Nguyen, L. T., Hoang, T. T., and Vogel, H. J. (2004) *Biochemistry* **43**, 2558-2568
37. Ogawa, Y., and Tanokura, M. (1984) *J. Biochem.* **95**, 19-28
38. Tanokura, M., and Yamada, K. (1984) *J. Biochem.* **95**, 643-649
39. Milos, M., Schaer, J.-J., Comte, M., and Cox, J. A. (1986) *Biochemistry* **25**, 6279-6287

40. Tanokura, M., and Yamada, K. (1993) *J. Biol. Chem.* **268**, 7090-7092
41. Potter, J. D., Hsu, F.-J., and Pownall, H. J. (1977) *J. Biol. Chem.* **252**, 2452-2454
42. Yamada, K., and Kometani, K. (1982) *J. Biochem.* **92**, 1505-1517
43. Imaizumi, M., Tanokura, M., and Yamada, K. (1987) *J. Biol. Chem.* **262**, 7963-7966
44. Tanokura, M., Imaizumi, M., and Yamada, K. (1986) *FEBS Lett.* **209**, 77-82
45. Tanokura, M., and Yamada, K. (1987) *Biochemistry* **26**, 7668-7574
46. Klee, C. B. (1977) *Biochemistry* **16**, 1017-1024
47. Wolff, D. J., Poirier, P. G., Brostrom, C. O., and Brostrom, M. A. (1977) *J. Biol. Chem.* **252**, 4108-4117
48. Cox, J. A., Ferraz, C., Demaile, J. G., Perez, R. O., van Tuinen, D., and Marme, D. (1982) *J. Biol. Chem.* **257**, 10694-10700
49. Dudev, T., and Lim, C. (2007) *Acc. Chem. Res.* **40**, 85-93

#### FOOTNOTES

\*This research was supported by Grants-in-aid for Scientific Research on Priority Areas “Structures of Biological Macromolecular Assemblies” from the Ministry of Education, Culture, Sports, Science and Technology of Japan.

§Present address: Organization of Advanced Science and Technology, Kobe University, 1-1 Rokkodai, Nada, Kobe 657-8501, Japan

<sup>1</sup>Abbreviations: BChl, bacteriochlorophyll; LH, light-harvesting; RC, reaction center; ITC, isothermal titration calorimetry; CD, circular dichroism; OG, *n*-octyl- $\beta$ -D-glucopyranoside; EDTA, ethylenediamine tetraacetic acid

#### FIGURE LEGENDS

**FIGURE 1. Absorption spectra of the Ca<sup>2+</sup>-depleted LH1-RC complex (B880) from *Tch. tepidum* and the spectral changes induced by the addition of various divalent cations (20 mM) to the B880.** Inset is the expanded view of the LH1 *Q<sub>y</sub>* region: B880 (black), Mg<sup>2+</sup> (blue), Ca<sup>2+</sup> (red), Sr<sup>2+</sup> (magenta), Ba<sup>2+</sup> (green) and Cd<sup>2+</sup> (purple).

**FIGURE 2. Spectral change of the absorptions after the addition of Ca<sup>2+</sup> at various concentrations to the B880 complex of *Tch. tepidum*.** All samples were incubated at 4 °C overnight. The change of wavelength for the LH1 *Q<sub>y</sub>* absorption peak is shown in the inset as a function of the Ca<sup>2+</sup> concentration. Concentration of the LH1 subunit was 16  $\mu$ M and residual EDTA in the solution was lower than 1 nM.

**FIGURE 3. Time profile of the absorption change at 937nm after addition of 5 mM Ca<sup>2+</sup> to the B880 complex of *Tch. tepidum*.** Concentration of the LH1 subunit was 7  $\mu$ M and the measurement was conducted at 25 °C. The dotted line was obtained by pseudo first-order kinetic analysis using Eq. 1. Inset shows a plot of apparent rate constants at different Ca<sup>2+</sup> concentrations.

**FIGURE 4. Comparison between the measured and calculated absorption changes at selected wavelengths as a function of the Ca<sup>2+</sup> concentration.** The experimental data were analyzed by the non-linear least-square fitting using Eq. 2.

FIGURE 5. **Isothermal titration calorimetric result of  $\text{Ca}^{2+}$ -binding to the LH1 complex.** (A) ITC titrations of 50 mM  $\text{CaCl}_2$  into 250  $\mu\text{M}$  of the LH1 B880  $\alpha\beta$ -subunits at 25 °C. (B) Binding isotherm of the titration as a function of  $\text{Ca}^{2+}/\alpha\beta$ -subunit ratio, solid line represents the best fit to a one-site model with the fitting parameters given in the text. The inset shows an expansion of the thermogram for the 1<sup>st</sup> injection.

FIGURE 6. **CD spectra for the B915 (broken line) and B880 (solid line) complexes from *Tch. tepidum* in the 400-1000 nm region and 200-280 nm region (inset).** The spectra were normalized with respect to the absorption bands at 514 nm and 280 nm, respectively.

FIGURE 7. **Effects of EDTA and metal cations on the absorption spectra of the chromatophores from *Tch. tepidum*.** Inset shows an expanded view of the LH1  $Q_y$  region: Native (solid line), 500 mM of  $\text{Ca}^{2+}$  (dotted line) and  $\text{Mg}^{2+}$  (dotted and dashed line), and 20 mM of EDTA (dashed line).

FIGURE 8. **Comparison of the amino acid sequences of LH1  $\alpha$ - and  $\beta$ -polypeptides from *Tch. tepidum* and *Ach. vinosum* (6, 7).** The sequences are aligned relative to the BChl *a*-coordinating histidine residues (shadow fonts). Acidic amino acid residues in the C-termini of  $\alpha$ -polypeptides and N-termini of  $\beta$ -polypeptides are indicated by bold fonts and a deletion in the *Tch. tepidum*  $\alpha$ -polypeptide is indicated by arrow. Underlined regions represent hydrophobic membrane-spanning domains predicted by SOSUI (<http://bp.nuap.nagoya-u.ac.jp/sosui/>).

Figure 1

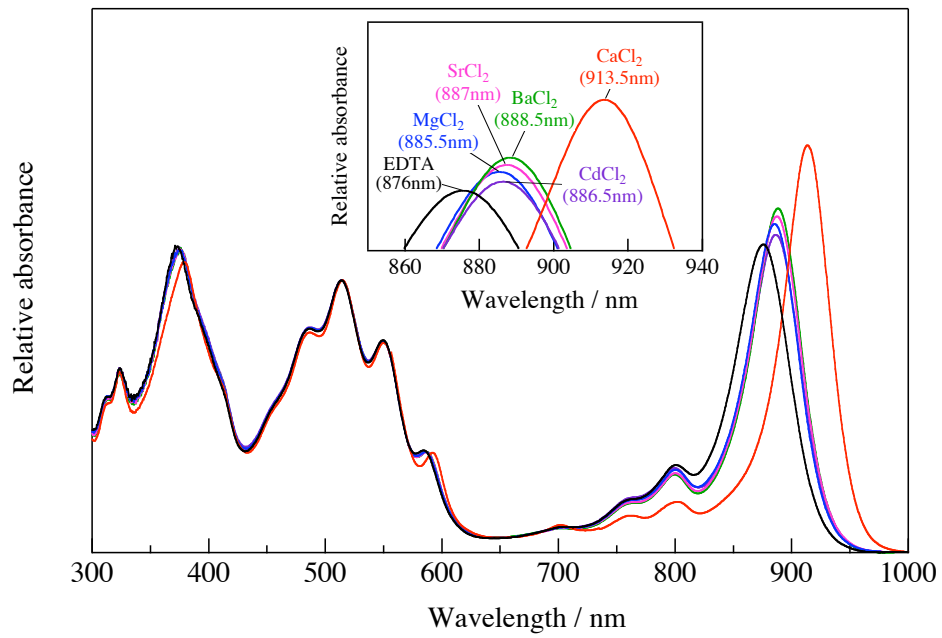


Figure 2

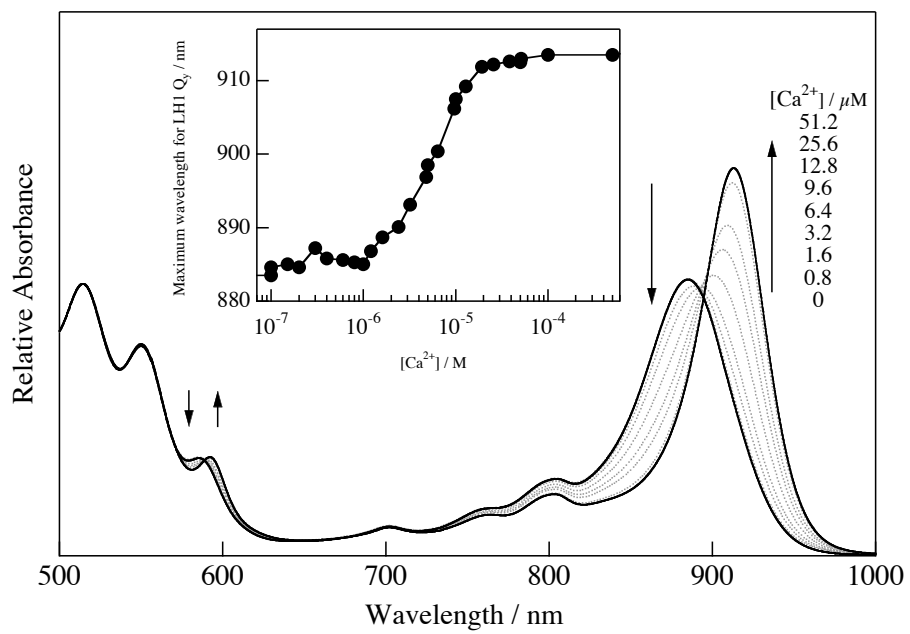


Figure 3

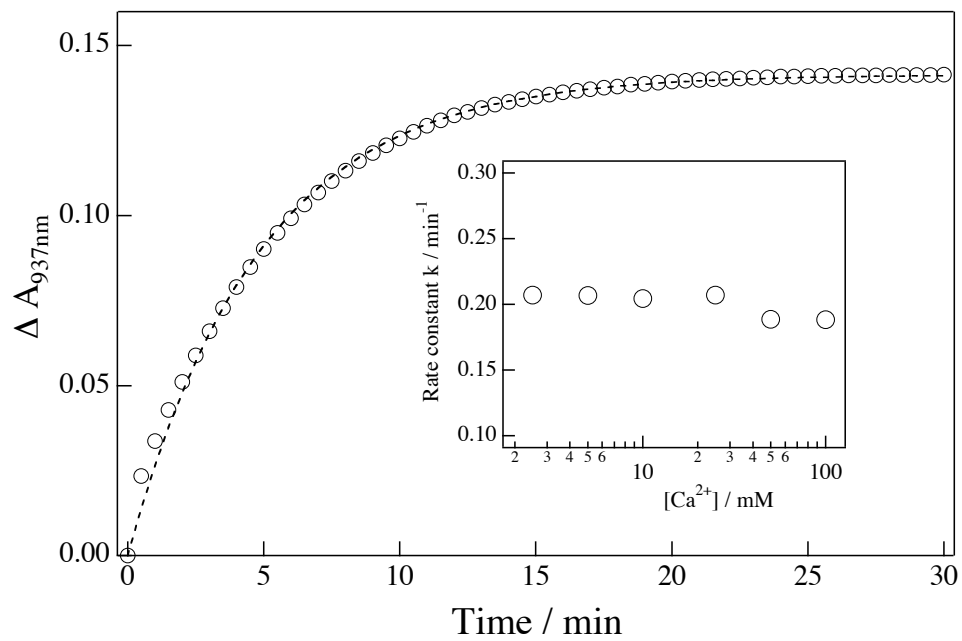


Figure 4

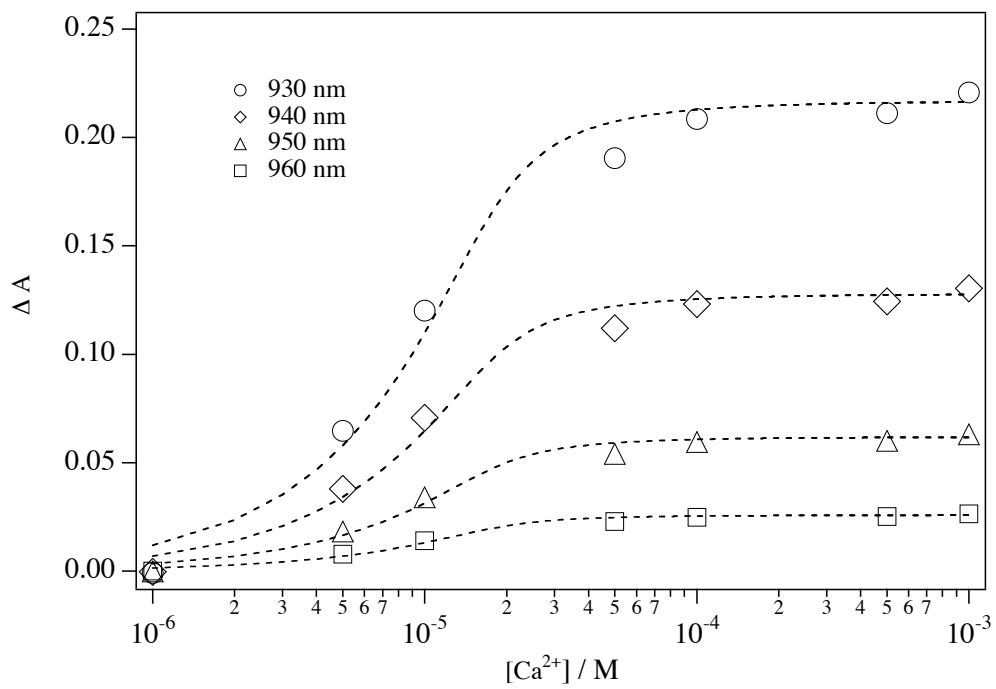


Figure 5

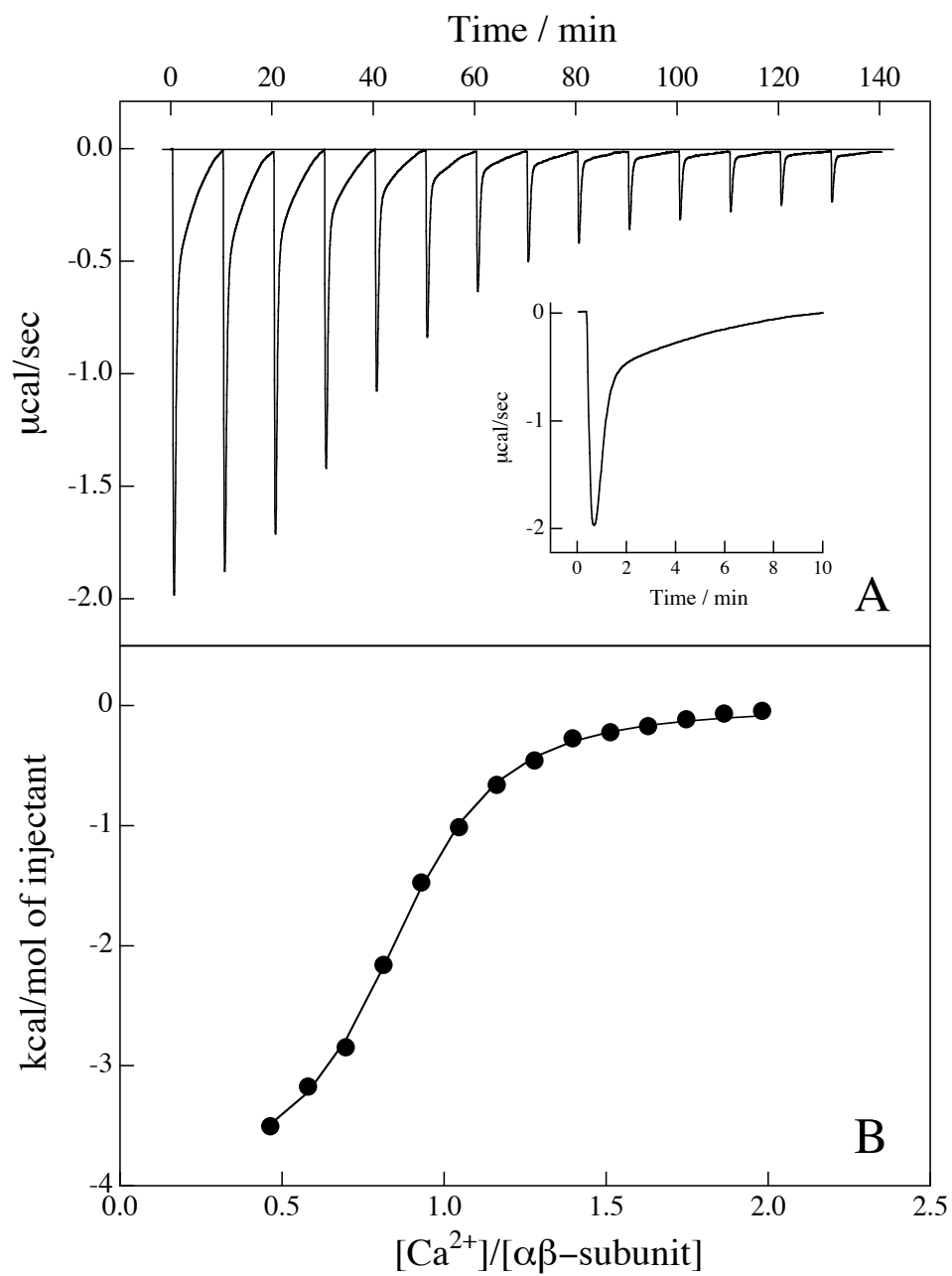


Figure 6

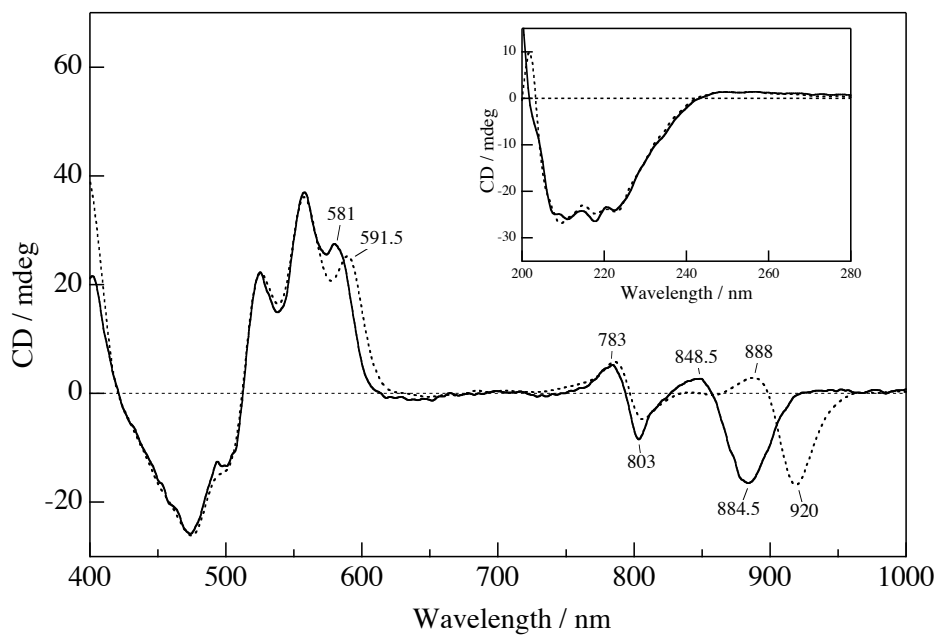
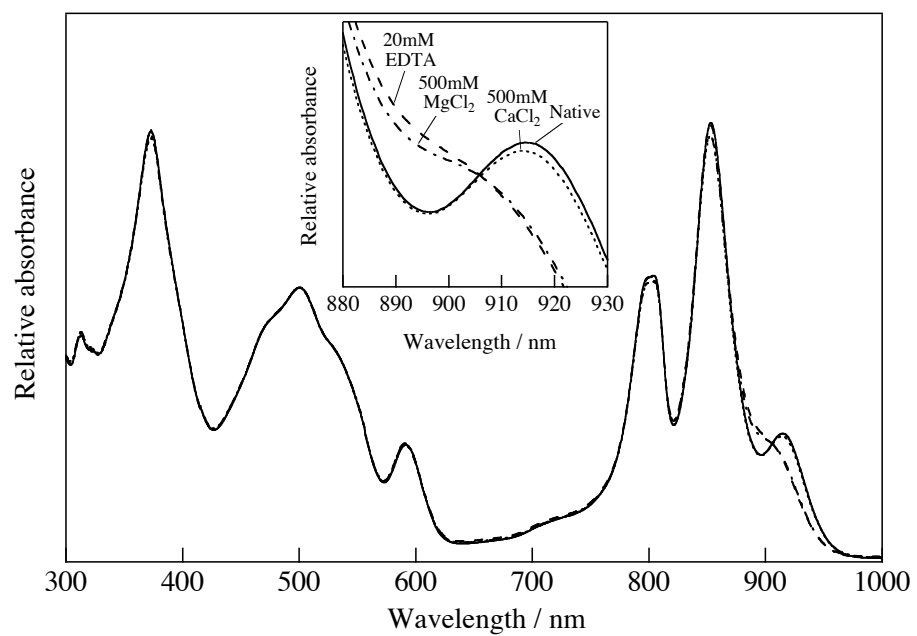


Figure 7



## Figure 8

LH1- $\alpha$

*Tch. tepidum* MFTMNANLYKIWLILDPRRVLVSIVAFQIVLGLLIHMIVLST-**DL**NWL**DD**NIPVSYQALGKK

*Ach. vinosum* MSPDLWKIWLLVDPRRILIAVFAFLTVLGLAIHMILLST**AE**FNW**LE**DGVPAA

LH1- $\beta$

*Tch. tepidum* AEQKSLTGLT**DDE**AK**E**FHAIFMQSMYAWFGLVVIAHLLLAWLYRPWL

*Ach. vinosum* NSSMTGLT**EQE**AQ**E**FHGIFVQSMTAFFGIVVIAHILAWLWRPWL